

pocampus but not from the striatum, was responsible for the trophic effects on Remak's ganglion. The trophic activity in the dialysate seen in the first 2 hours after implantation of the probe into the hippocampus is probably due to the probe-induced mechanical damage of the tissue, affecting an already existing pool of trophic bioactivity in the hippocampus.

After injection of kainic acid, all animals exhibited the typical complex stages of convulsions, lasting the entire period of the experiment. Kainic acid significantly increased the same kind of trophic activity in hippocampal dialysates, as demonstrated by an increased nerve fiber outgrowth in Remak's ganglion. Again, the kainic acid effect was region-specific and thus not found in the striatum. In marked contrast to kainic acid, pentylentetrazol did not increase trophic activity in hippocampal dialysates, despite the fact that animals exhibited massive generalized seizures 3 to 5 min after injection. The lack of ability of pentylentetrazol to induce an increased activity in hippocampal dialysates might possibly be explained by the shorter excitatory stimulation and lack of neuronal degeneration. Alternatively, the two convulsant drugs might act through different mechanisms.

Taken together, our experiments demonstrate that neurotrophic activity can be captured from the extracellular space by in vivo dialysis in the hippocampus, but not striatum, of awake rats. The trophic activity is not compatible with that of known neurotrophins or other trophic factors, is regionally specific, and is increased by mechanical and certain convulsant treatments.

REFERENCES AND NOTES

1. T. Ebendal, *J. Neurosci. Res.* **32**, 461 (1992); Y. A. Barde, *Prog. Growth Factor Res.* **2**, 237 (1990); P. A. Lapchak, D. M. Araujo, F. Hefti, *Rev. Neurosci.* **3**, 1 (1992); R. Levi-Montalcini and P. U. Angeletti, *Physiol. Rev.* **48**, 534 (1968); R. Levi-Montalcini, *Biochem. Biophys. Res. Commun.* **7**, 681 (1967); R. Levi-Montalcini, L. Aloe, E. Alleva, *Prog. Neuroendocrinol.* **3**, 1 (1990).
2. P. Ernfors, C. Wetmore, L. Olson, H. Persson, *Neuron* **5**, 511 (1990); C. M. Gall, *Trends Pharmacol. Sci.* **13**, 401 (1992); C. Ayer-LeLievre et al., *Science* **240**, 1339 (1988).
3. C. Wetmore, Y. Cao, R. F. Pettersson, L. Olson, *Proc. Natl. Acad. Sci. U.S.A.* **88**, 9843 (1991); *J. Histochem. Cytochem.* **41**, 521 (1993).
4. T. Ebendal, A. Jordell-Kylberg, S. Söderström, *Zoon* **6**, 235 (1978); T. Ebendal, in *Nerve Growth Factors*, R. A. Rush, Ed. (Wiley, Chichester, UK, 1989), pp. 81–93.
5. For all release experiments, a microdialysis probe (Carnegie Medicine, Stockholm, Sweden) with a molecular cutoff of 100,000 daltons was used. To determine recovery in vitro, the probe was immersed in a range of concentrations of purified NGF and perfused with Ringer solution (147 mM NaCl, 4 mM KCl, and 2.3 mM CaCl₂) at a flow rate of 2 or 0.5 μ l/min, starting with the lowest concentration of NGF. Samples were collected for 60 min on ice and subsequently frozen at -20°C . NGF concentrations were determined by bioassay using chick embryo spinal and sympathetic ganglia (4) or by EIA (6). At a flow rate of 2 μ l/min, NGF activity was detected in the dialysate from stock solutions

of 2 μ g/ml and 300 ng/ml (0.35 to 0.08 scoring units), corresponding to a recovery of 3 to 5%. When the flow rate was lowered to 0.5 μ l/min, NGF could be captured from stock solutions of 3 ng of NGF per milliliter, with a recovery of 12 to 35% as determined by EIA (6).

6. S. Söderström, F. Hallböök, C. F. Ibáñez, H. Persson, T. Ebendal, *J. Neurosci. Res.* **27**, 665 (1990).
7. A. Shintani et al., *Biochem. Biophys. Res. Commun.* **194**, 1500 (1993); S. Söderström and T. Ebendal, *Neurosci. Lett.* **189**, 5 (1995). An NT-3 EIA calibration curve is shown in Fig. 3A.
8. Trophic activity was determined (in scored BU) in a bioassay with chick embryo spinal, sympathetic, Remak's, ciliary, and nodose ganglia (4). Ganglia were dissected from 8- to 9-day-old chicken embryos. Several ganglia were put in a culture dish in a 50-ml collagen matrix (4). Incubation was carried out for 2 days at 37°C under standard cell culture conditions. Fiber outgrowth was examined with dark-field or phase-contrast microscopy. Ganglia and fiber outgrowth patterns were drawn on a blind basis by one investigator. To score the different outgrowth intensities, the drawings were scored blindly by a second investigator on a scale of 0 to 3. This scale defines 3.0 as the maximal outgrowth seen in dorsal root or sympathetic ganglia in the presence of optimal concentrations of NGF. In the present experiments, maximal scores obtained with addition of brain dialysates to Remak's ganglion were 2.0. Most scores were in the 0.0 to 1.0 range. By counting of neurites or estimation of neurite densities when larger numbers had formed, or both, the scoring in this range could be done in increments of 0.2. All neurotrophins have been tested in the bioassay with different ganglia (P. Ernfors et al., *Proc. Natl. Acad. Sci. U.S.A.* **87**, 5454, 1990).
9. To determine the in vivo release of trophic substances, microdialysis probes were implanted with the use of coordinates calculated from the atlas of

Paxinos and Watson [S. Paxinos and C. Watson, *The Rat Brain in Stereotaxic Coordinates* (Academic Press, San Diego, CA, 1986)] Probes were placed in the hippocampus (bregma, -4.0 ; lateral, $+5.0$; angle, 45° to the midline; and depth, -5.0) or striatum (bregma, $+0.5$; lateral, $+3.0$; and depth, -5.0) and perfusion was started with a flow rate of 0.5 μ l/min with sterile Ringer solution. All in vivo perfusion experiments were done under sterile conditions in a laminar flow bench. Perfusates were usually collected over 2-hour periods, generating four 60- μ l 2-hour samples per animal. Samples were collected at room temperature and frozen. The animal setup, tubings, and the chosen flow rate allowed material in the probe to reach the collection vials in 20 min. Known neurotrophins are stable for long periods of time (weeks to months) at temperatures up to body temperature.

10. To induce release of trophic substances, the convulsive drugs kainic acid [12 mg per kilogram of body weight, intraperitoneal (i.p.); $n = 13$ rats] and pentylentetrazol (50 mg per kilogram of body weight, i.p.; $n = 5$ rats) were injected 4 hours after implantation of the microdialysis probes. Statistical evaluations were carried out using one-way ANOVA with subsequent Fisher's protected least significant difference posthoc test comparison.
11. T. Ebendal, A. Tomac, B. J. Hoffer, L. Olson, *J. Neurosci. Res.* **40**, 276 (1995).
12. T. Ebendal, unpublished observations.
13. We thank T. Hökfelt for carefully reading this manuscript. Supported by the Austrian Scientific Research Fund, the Swedish Medical Research Council, the U.S. Public Health Service, and the Swedish Natural Science Research Council. We thank K. Igarashi, Takeda Chemical Industries, Japan, for supply of antibody 3W3 to NT-3. Human rNT-3 was purchased from Austral Biologicals, CA, USA.

23 January 1995; accepted 26 April 1995

Activation of Yeast PBS2 MAPKK by MAPKKKs or by Binding of an SH3-Containing Osmosensor

Tatsuya Maeda,* Mutsuhiro Takekawa, Haruo Saito†

The role of mitogen-activated protein (MAP) kinase cascades in integrating distinct upstream signals was studied in yeast. Mutants that were not able to activate PBS2 MAP kinase kinase (MAPKK; Pbs2p) at high osmolarity were characterized. Pbs2p was activated by two independent signals that emanated from distinct cell-surface osmosensors. Pbs2p was activated by MAP kinase kinases (MAPKKKs) Ssk2p and Ssk22p that are under the control of the SLN1-SSK1 two-component osmosensor. Alternatively, Pbs2p was activated by a mechanism that involves the binding of its amino terminal proline-rich motif to the Src homology 3 (SH3) domain of a putative transmembrane osmosensor Sho1p.

A conserved MAP kinase cascade that functions in many eukaryotic signal transduction pathways consists of a MAP kinase (MAPK), a MAPK kinase (MAPKK), and a MAPKK kinase (MAPKKK) (1). The cascades of three kinases serve as intermediaries between cell-surface receptors and cyto-

solic and nuclear effectors. However, the functional significance of having three kinases in a cascade is not clear. Although the three kinases amplify a signal along the pathway, it is also possible that the series of protein kinases provides a mechanism for integrating signals from distinct receptors. Here, we demonstrate a case in which a single MAPKK integrates two distinct upstream signals. One of the activation mechanisms involves an interaction between the SH3 domain of a transmembrane molecule (a putative osmosensor) and a Pro-rich region in the Pbs2p MAPKK.

In the yeast *Saccharomyces cerevisiae*, ex-

Division of Tumor Immunology, Dana-Farber Cancer Institute, and Department of Biological Chemistry and Molecular Pharmacology, Harvard Medical School, Boston, MA 02115, USA.

*Present address: Department of Viral Oncology, Cancer Institute, Kami-Ikebukuro, Toshima-ku, Tokyo 170, Japan.

†To whom correspondence should be addressed at Dana-Farber Cancer Institute, 44 Binney Street, Boston, MA 02115, USA.

posure to extracellular fluid of high osmolarity activates a MAPK cascade that includes the *PBS2* MAPKK and the *HOG1* MAPK (2). The MAPKKK component of this MAPK cascade is not known, but signaling elements further upstream in the pathway have been identified. A two-component system, composed of the transmembrane sensor histidine kinase *Sln1p* (3) and the cytoplasmic response regulator *Ssk1p*, appears to be an osmosensor that regulates the *PBS2-HOG1* MAPK cascade (4). *Sln1p* serves as a negative regulator of the *PBS2-HOG1* pathway. Disruption of *SLN1* is lethal because of inappropriate activation of the *PBS2-HOG1* pathway. Therefore, it was possible to identify elements necessary to transduce signals between *Sln1p* and *Hog1p* by isolating extragenic suppressor mutants of *sln1Δ* or *sln1^{ts}* (ts, temperature-sensitive).

We thus demonstrated that mutations in the *SSK1*, *PBS2*, or *HOG1* genes suppressed *sln1Δ* (4). We cloned another extragenic suppressor gene, *SSK2*, to identify the predicted MAPKKK in this signal pathway. Nucleotide sequence determination of *SSK2* indicated that it encoded a protein with a COOH-terminal domain (amino acid position 1266 to the COOH-terminus) (Fig. 1A) that is similar to MAPKKKs such as *MEKK* (37% identity in the kinase domain), *Ste11p* (40%), and *Bck1p* (39%). In contrast, the long, NH₂-terminal noncatalytic domain of about 1200 amino acids has no similarity to these MAPKKKs.

Further analysis, however, indicated that *Ssk2p* is not solely responsible for activation of the *PBS2-HOG1* pathway: *ssk2Δ* mutant cells activated tyrosine phosphorylation of *Hog1p* in a *PBS2*-dependent manner (5). One possible explanation for this activation was the presence of another gene that was functionally the same as *SSK2*. We used low stringency Southern (DNA) hybridization of yeast genomic DNA with an *SSK2* probe to identify an *SSK2*-related gene termed *SSK22*. Sequence comparison revealed that *SSK2* and *SSK22* are similar both in their COOH-terminal kinase domain (69% identity) and in the NH₂-terminal noncatalytic domain (47% identity) (Fig. 1A). We examined the possibility that both kinases can activate the *PBS2-HOG1* pathway. Kinases in the MAPKKK family can be constitutively activated by elimination of their NH₂-terminal noncatalytic domains (6). Thus, we constructed NH₂-terminal deletion mutants *SSK2ΔN* and *SSK22ΔN* and placed them under the control of the inducible *GAL1* promoter (7). Protein immunoblot analysis demonstrated that expression of either *SSK2ΔN* or *SSK22ΔN* induced tyrosine phosphorylation of *Hog1p* in a *PBS2*-dependent manner (Fig. 1B). Expression of either *SSK2ΔN* or *SSK22ΔN* was lethal to the host cells, and this lethality was complete-

ly abrogated by deletion mutations in either the *PBS2* or *HOG1* gene, but not in the *SSK1* gene (5). Furthermore, a two-hybrid analysis (8) indicated that both *Ssk2p* and *Ssk22p* can interact with *Ssk1p* (in the case of *Ssk2p*, this interaction required only the NH₂-terminal nonkinase domain) (5). We conclude that the signal generated by the *SLN1-SSK1* two-component osmosensor is transduced to a MAPK cascade that is composed of *Ssk2p*

or *Ssk22p*, *Pbs2p*, and *Hog1p*.

If *Ssk2p* and *Ssk22p* are the only means of activating *Pbs2p*, then *ssk2Δ ssk22Δ* double mutants should be incapable of inducing *Pbs2p*-mediated tyrosine phosphorylation of *Hog1p*, and such double mutants should be as sensitive to high osmolarity (*Osm^S*) as *pbs2Δ* mutants (Fig. 2, A and B). However, treatment of *ssk2Δ ssk22Δ* double mutants with media of high osmolarity induced tyrosine phosphorylation of *Hog1p* nearly as

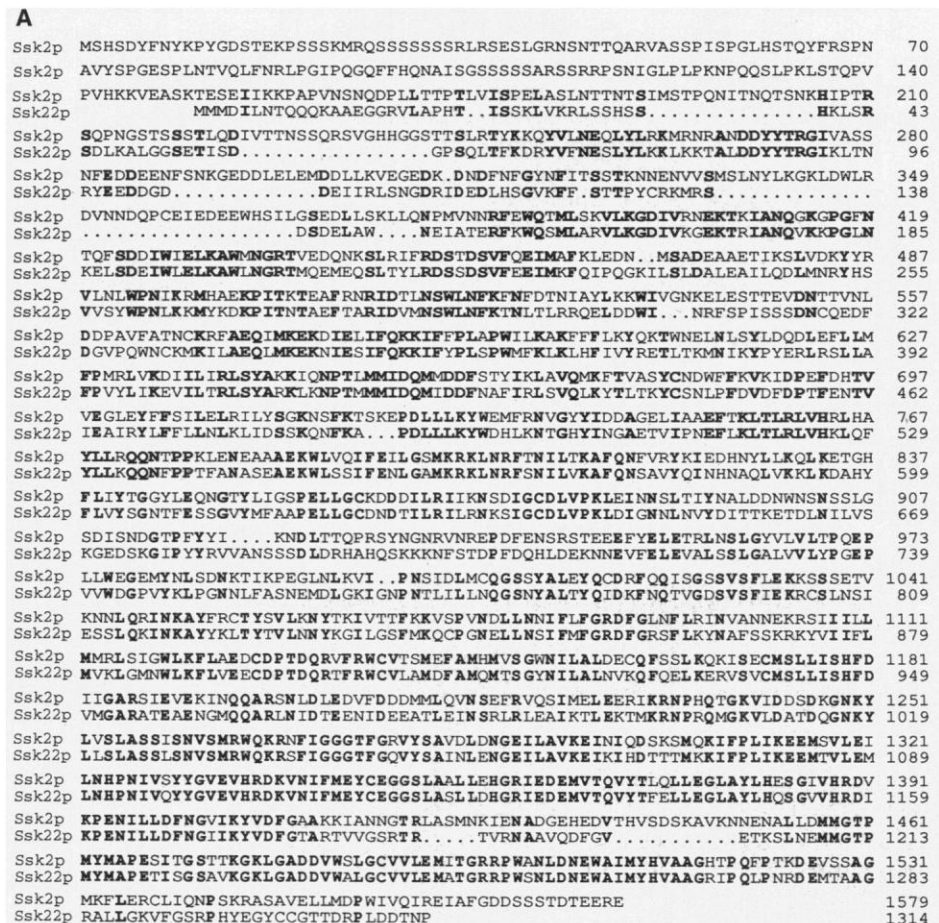
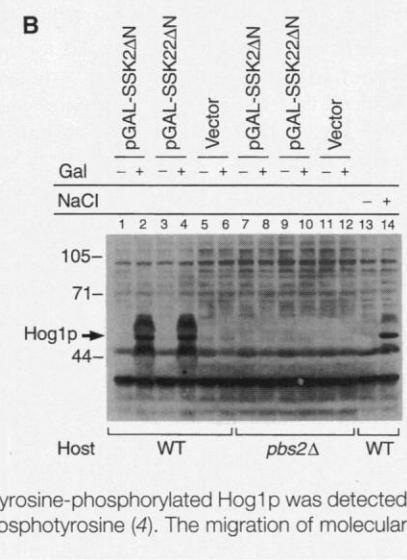


Fig. 1. Two MAPKKKs that activate *Pbs2p*. **(A)** Deduced amino acid sequences of *Ssk2p* and *Ssk22p* (14). The *SSK2* gene was cloned by complementation of an *sln1-ts4 ssk2* mutant (4) from a Yc50-based genomic library. Identical amino acid residues between *Ssk2p* and *Ssk22p* are highlighted in boldface. *SSK22* corresponds to the open reading frame YCR73c on chromosome III (21) (GenBank accession number X59720). The GenBank accession number for *SSK2* is L41927. **(B)** *PBS2*-dependent *Hog1p* tyrosine phosphorylation induced by the expression of the catalytic domain of *Ssk2p* (*pGAL-SSK2ΔN*) or *Ssk22p* (*pGAL-SSK22ΔN*) (7). These plasmids were individually transformed into either wild-type (WT) strain TM101 (*MATα ura3 leu2 his3*) or its *pbs2Δ* (*pbs2::LEU2*) derivative TM261. Gene expression in cells grown in synthetic complete (SC) medium with raffinose (20 g/liter) was induced with galactose (4). Samples were taken before (–) the addition of galactose or 1 hour later (+) (lanes 1 through 12). Wild-type cells were treated with 0.4 M NaCl for 0 min (–) or 10 min (+) (lanes 13 and 14). Tyrosine-phosphorylated *Hog1p* was detected by immunoblotting with monoclonal antibody 4G10 to phosphotyrosine (4). The migration of molecular size markers is shown to the left in kilodaltons.



efficiently as in wild-type cells (Fig. 2A), and *ssk2Δ ssk22Δ* double mutants were resistant to the effects of high osmolarity (Osm^R) (Fig. 2B). Thus, there must exist an alternative mechanism to activate Pbs2p without Ssk2p or Ssk22p. Because no other gene similar to SSK2 or SSK22 could be identified (5), we conducted a mutant screening on the basis of the assumption that simultaneous inactivation of SSK2, SSK22, and a gene involved in the alternative activation mechanism would create an Osm^S phenotype (9).

Briefly, *ssk2Δ ssk22Δ* double mutants were mutagenized, and Osm^S mutants were selected. Among the Osm^S mutants, those that could be made Osm^R by transformation with either SSK2⁺ or SSK22⁺ were identified. This screening yielded two mutants (OS-13 and OS-121), each of which harbored a mutation that was synthetically Osm^S with *ssk2 ssk22*. The first mutant, OS-13, had a missense mutation in the PBS2 gene. The second mutant, OS-121, had a mutation (*sho1-121*) in a gene we call SHO1 (synthetic, high osmolarity-sensitive).

The SHO1 gene was cloned by complementation of *sho1-121* with a genomic DNA library (10). SHO1 encodes a protein composed of 367 amino acids (Fig. 2C). A hydropathy plot (11) of the Sho1p amino acid sequence (Fig. 2E) suggested that its NH₂-terminal region contains four closely packed hydrophobic transmembrane peptides. Because there is no signal sequence at the NH₂-terminus, both the NH₂- and COOH-termini of Sho1p are expected to be located in the cytoplasm. Furthermore, the COOH-terminal region of Sho1p contains an SH3 domain (Fig. 2D). The SH3 domain is a module that appears in numerous signal transduction proteins and binds Pro-rich motifs (12). These structural features suggest that Sho1p is an alternative osmosensor in yeast.

To study the role of Sho1p in the activation of Pbs2p, we generated a disruption mutant of SHO1 (10). The *sho1Δ* mutation alone had little effect on the high osmolarity-induced tyrosine phosphorylation of Hog1p (Fig. 2A), and the *sho1Δ* single mutant cells were Osm^R (Fig. 2B). Furthermore, *ssk2Δ sho1Δ* and *ssk22Δ sho1Δ* double mutants were still capable of phosphorylating Hog1p on tyrosine (Fig. 2A) and were Osm^R (Fig. 2B). The extent of tyrosine phosphorylation of Hog1p in *ssk2Δ sho1Δ* is somewhat smaller than in *ssk22Δ sho1Δ*, which suggests that the activity or expression (or both) of Ssk22p is weaker than that of Ssk2p. More importantly, however, the combination of the three mutations (*ssk2Δ*, *ssk22Δ*, and *sho1Δ*) completely abolished tyrosine phosphorylation of Hog1p (Fig. 2A), and the triple mutant was Osm^S (Fig. 2B). Thus, Sho1p appears to be a component of an

alternative pathway that activates Pbs2p in response to high osmolarity.

The presence of an SH3 domain in Sho1p suggested that it would bind to a target protein that contains a Pro-rich motif. The physiologically relevant target of the Sho1p SH3 domain was identified as Pbs2p itself through the characterization of the second synthetic Osm^S mutant OS-13. By complementation analysis and gene cloning, OS-13 was found to harbor a mutation (*pbs2-13*) in the PBS2 gene (13). The phenotypic effect of the *pbs2-13* allele was manifested only when it was accompanied by both *ssk2* and *ssk22* mutations (Fig. 3A). In contrast, most other *pbs2* mutations—for example, *pbs2^{K/M}* in which Lys³⁵⁹ is mutated to Met—confer sensitivity to high osmolarity by themselves. This similarity of the *pbs2-13* and *sho1Δ* mutations (their phenotypes are uncovered only in the presence of *ssk2 ssk22* mutations) suggests that the *pbs2-13* mutant is defective only in the branch of the signal pathway activated by Sho1p. The *pbs2-13* mu-

tation was a single amino acid substitution of Ser for Pro at position 96 (Fig. 3B). This Pro residue resides within a Pro-rich sequence (KPLPPLPVA) (14) that is reminiscent of known SH3-binding sites (Fig. 3C).

Therefore, we used two-hybrid analysis (8) to test the possibility that the Sho1p SH3 domain binds to the Pbs2p Pro-rich motif. The SH3 domain of Sho1p interacted with wild-type Pbs2p, but not with the *pbs2-13* mutant protein (Fig. 3D). Thus, the binding of Sho1p to Pbs2p appears to activate Pbs2p without the involvement of Ssk2p or Ssk22p. Conversely, activation of Pbs2p by Ssk2p or Ssk22p appears not to require the SH3 domain binding site, because *pbs2-13* mutants are Osm^R as long as either SSK2 or SSK22 is intact. Activation by interaction with SH3-containing proteins may occur in a subset of MAPKKs, because several MAPKKs also have Pro-rich motifs in their NH₂-terminal region (yeast Mkk1p: PAPPPLP; yeast Mkk2p: PVPPPLPP; human MKK3: PPAPNPTPP) (14–16).

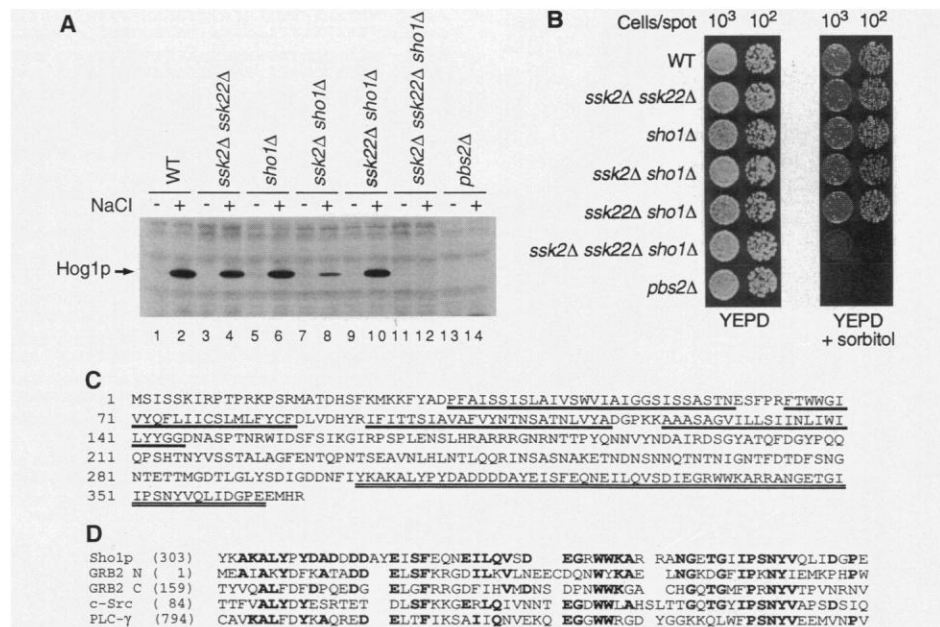


Fig. 2. SH3-containing transmembrane osmosensor Sho1p. (A) High osmolarity-induced Hog1p tyrosine phosphorylation in various mutant strains. Strains of the indicated genotypes (22) were grown in YEPD medium [yeast extract (10 g/liter), tryptone (20 g/liter), and glucose (20 g/liter)], and when absorbance at 600 nm was between 0.4 and 0.5, cells were collected before (–) or 5 min after (+) the addition of NaCl to a final concentration of 0.4 M. Tyrosine phosphorylated Hog1p was visualized as in Fig. 1B. (B) Sensitivity to high osmolarity of various mutant strains. About 10³ or 10² cells grown in YEPD medium were spotted on YEPD plates with or without 1.5 M sorbitol and incubated for 2 days at 30°C. (C) Deduced amino acid sequence of Sho1p. Putative transmembrane segments are highlighted by a single underline, and an SH3 domain is indicated by a double underline. SHO1 corresponds to the open reading frame YER118c on chromosome V. The GenBank accession number for the SHO1 nucleotide sequence is L41926. (D) Comparison of SH3 domain sequences. Amino acid residues identical to those in Sho1p are highlighted by boldface type. PLC-γ, phospholipase C-γ. (E) Hydropathy plot of Sho1p (11). Four putative transmembrane segments (I to IV) are indicated. A scanning window of 11 amino acids was used.

By analogy with other MAPKKKs, Ssk2p and Ssk22p are likely to activate Pbs2p by phosphorylation of Ser⁵¹⁴ and

Thr⁵¹⁸ within the kinase domain. To examine whether the Sho1p-mediated activation of Pbs2p also requires these phospho-

phorylation events, we mutated both phosphorylation sites to Ala (*pbs2^{S514 T518}*). The *pbs2^{S514 T518}* mutant allele could not complement *pbs2Δ* in any host background (Fig. 3A). Therefore, unless these amino acid substitutions cause irreversible conformational damage (17), we conclude that phosphorylation of these sites is required for Sho1p-mediated activation of Pbs2p. The Sho1p binding might induce autophosphorylation of Pbs2p at the activating phosphorylation sites or it might recruit an unidentified MAPKKK that activates Pbs2p.

The signal flow in the yeast response to high osmolarity is shown schematically in Fig. 4A. We propose that both Sln1p and Sho1p are transmembrane osmosensors that regulate the PBS2-HOG1 pathway. To test if the two osmosensors have different response characteristics, we compared two mutant strains: in the *ssk2Δ ssk22Δ* mutant, only the Sho1p-dependent pathway is available, whereas in the *sho1Δ ssk22Δ* mutant, only the Sln1p-dependent pathway is active. Tyrosine phosphorylation of Hog1p in the *ssk2Δ ssk22Δ* mutant was almost undetectable at or below a NaCl concentration of 200 mM, but at a concentration of 300 mM there was a nearly maximal response. In the *sho1Δ ssk22Δ* mutant, in contrast, the intensity of tyrosine phosphorylation of Hog1p gradually increased as the NaCl concentration was raised from 100 mM to 600 mM (Fig. 4B). With 300 mM NaCl, maximal response took 3 to 5 min in the *ssk2Δ ssk22Δ* mutant, whereas a peak was reached within 1 min in the *sho1Δ ssk22Δ* mutant (Fig. 4C). The two osmosensors with different concentration dependency and time course may be needed for optimal adaptation to a rapidly fluctuating osmotic environment. The mammalian MAPKs p38 and JNK1 can functionally complement yeast *hog1* mutations (18). These MAPKs are parts of mammalian MAPK cascades that are activated by various stresses, including treatment with media of high osmolarity (16, 19). Thus, it is possible that mammalian cells also use similar upstream mechanisms.

Fig. 3. Interaction between the SH3 domain of Sho1p and the Pro-rich motif of Pbs2p. (A) Effects on the sensitivity to osmolarity of a *pbs2-13* mutant allele in combination with mutations in *SSK2*, *SSK22*, and *SHO1*. Host cells were transformed with plasmids carrying various *PBS2* alleles (23). The transformants were cultured in SC medium minus Lys, and 10³ cells were spotted on YEPD plates with or without 1.5 M sorbitol. Pictures were taken after 2 days at 30°C. In the *pbs2^{KM}* mutant, the catalytically essential Lys is changed to Met; it lacks kinase activity. (B) The *pbs2-13* mutation changed Pro⁹⁶ to Ser within a conserved SH3-binding motif. (C) Comparison of SH3-binding motifs (24). The two essential Pro residues are enclosed in boxes. PI3K, phosphatidylinositol-3 kinase. (D) Two-hybrid analysis (25). The wild-type Pbs2p (*PBS2⁺*) interacted with the SH3 domain of Sho1p [SHO1(SH3)]. The mutant protein encoded by *pbs2-13* did not interact with the Sho1p SH3 domain. Proteins encoded by the control plasmids pLexA-RAS^{V12} and pACT-RAF interact with each other (20).

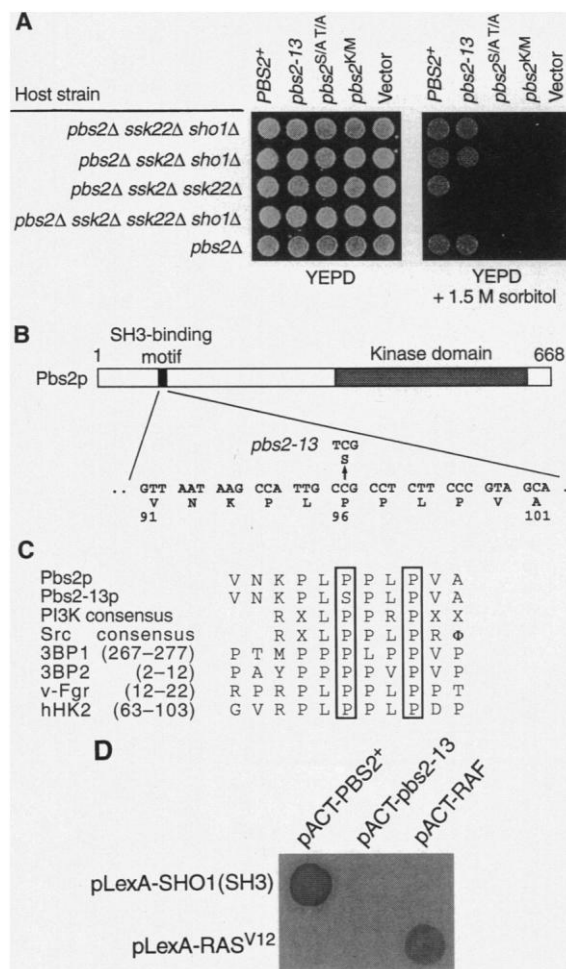
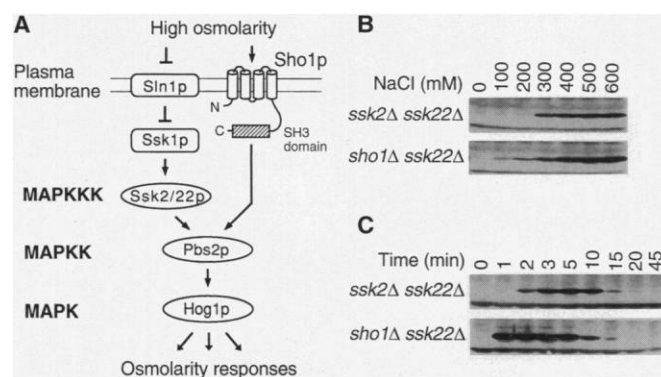


Fig. 4. Two distinct transmembrane osmosensors in yeast. (A) A schematized model of the yeast high osmolarity signal transduction pathway. Yeast cells have at least two independent transmembrane osmosensors, Sln1p and Sho1p. At low extracellular osmolarity, Sln1p (a transmembrane histidine kinase) phosphorylates and inhibits Ssk1p (a response regulator) (4). At high osmolarity, unphosphorylated Ssk1p activates Ssk2 or Ssk22p, probably through the direct interaction of Ssk1p and the NH₂-terminus of Ssk2 or Ssk22p. Activated Ssk2 or Ssk22p then activates Pbs2p by Ser-Thr phosphorylation, which in turn activates Hog1p by Thr-Tyr phosphorylation. At high osmolarity, another transmembrane osmosensor, Sho1p, also activates Pbs2p, through an interaction of the Sho1p SH3 domain and the Pbs2p SH3-binding site. This interaction alone may activate the *PBS2* kinase (perhaps by inducing Pbs2p autophosphorylation). However, it is also possible that the interaction of Sho1p with Pbs2p recruits another molecule that activates Pbs2p. (B) NaCl dependence of Hog1p tyrosine phosphorylation. NaCl was added at the indicated concentration to growing cultures of either TM295 (*MATa ura3 leu2 trp1 his3 ssk2::URA3 ssk22::LEU2*) or TM312 (*MATa ura3 leu2 trp1 his3 sho1::TRP1 ssk22::LEU2*). Five minutes after the addition of NaCl, cells were collected and tyrosine phosphorylated Hog1p was visualized by immunoblotting as in Fig. 1B. (C) Time course of Hog1p tyrosine phosphorylation. TM295 or TM312 cells were exposed to 300 mM NaCl for the time indicated, and tyrosine-phosphorylated Hog1p was detected.



REFERENCES AND NOTES

1. J. A. Cooper, *Curr. Biol.* **4**, 1118 (1994); R. J. Davis, *Trends Biochem. Sci.* **19**, 470 (1994); I. Herskowitz, *Cell* **80**, 187 (1995).
2. G. Boguslawski, *J. Gen. Microbiol.* **138**, 2425 (1992); J. L. Brewster, T. de Valoir, N. D. Dwyer, E. Winter, M. C. Gustin, *Science* **259**, 1760 (1993).
3. I. M. Ota and A. Varshavsky, *Science* **262**, 566 (1993).
4. T. Maeda, S. M. Wurgler-Murphy, H. Saito, *Nature* **369**, 242 (1994).
5. T. Maeda and H. Saito, unpublished data.
6. B. R. Cairns, S. W. Ramer, R. D. Kornberg, *Genes Dev.* **6**, 1305 (1992).
7. The DNA segments of *SSK2* (Met¹¹⁷³ to the COOH-terminus) or *SSK22* (Met⁹⁵¹ to the COOH-terminus) were cloned into a *GAL1* promoter expression plasmid pYES2 (vector; *URA3⁺* marker) to construct

- pGAL-SSK2ΔN and pGAL-SSK22ΔN, respectively.
8. C. T. Chien, P. L. Bartel, R. Sternglanz, S. Fields, *Proc. Natl. Acad. Sci. U.S.A.* **88**, 9578 (1991).
 9. Yeast strains TM252 (*MATa ura3 leu2 trp1 ssk2::LEU2 ssk22::LEU2*) and TM253 (*MATα ura3 leu2 his3 ssk2::LEU2 ssk22::LEU2*) were mutagenized with *N*-methyl-*N'*-nitro-*N*-nitrosoguanidine [C. W. Lawrence, *Methods Enzymol.* **194**, 273 (1991)]. About 57,000 colonies of mutagenized cells were grown on YEPD (yeast extract, peptone dextrose) plates and replica-plated onto YEPD + 1.5 M sorbitol. Complementation analyses of 72 high osmolarity-sensitive mutants resulted in six complementation groups, of which *pbs2* (20 mutants), *hog1* (12 mutants), and *gpd1* (1 mutant) were known osmosensitive genes. Three other complementation groups had 10, 7, and 3 mutants, respectively. The remaining mutants could not be grouped. To identify synthetic *Osm^S* mutants, we transformed each mutant with *SSK2* or *SSK22* carried on a single-copy plasmid vector. Synthetic *Osm^S* mutants would be rendered *Osm^R* by transformation with either of these genes. Two mutants, OS-13 and OS-121, met the criteria.
 10. OS-121 (*MATa sho1-121 ura3 leu2 trp1 ssk2::LEU2 ssk22::LEU2*) was transformed with a yeast genomic DNA library in YCp50 (*URA3⁺* marker). *Ura⁺* transformants were replica-plated onto YEPD + 1.5 M sorbitol, and *Osm^R* colonies were selected. Plasmids rescued from the *Osm^R* transformants contained either *SSK2* or *SHO1*. The location of *SHO1* in the cloned DNA segment was determined by deletion and complementation mapping. The complete nucleotide sequence of the smallest restriction fragment (a 2.3-kb Hind III to Xba I fragment) that could complement *sho1-121* was sequenced. The fragment contained a 1101-bp open reading frame. We disrupted the *SHO1* gene by replacing an internal Eco RV fragment (corresponding to amino acid positions 207 to 295) with *TRP1*.
 11. J. Kyte and R. F. Doolittle, *J. Mol. Biol.* **157**, 105 (1982).
 12. G. B. Cohen, R. Ren, D. Baltimore, *Cell* **80**, 237 (1995); T. Pawson, *Nature* **373**, 573 (1995).
 13. The *pbs2-13* allele was recovered by gap-filling [R. Rothstein, *Methods Enzymol.* **194**, 281 (1991)]. The *pbs2-13* mutation was located within a 336-bp Xcm I to Afl II fragment that corresponds to amino acid positions 13 through 124 of *Pbs2p*. The nucleotide sequence of this segment was determined for both *PBS2⁺* and *pbs2-13*.
 14. Abbreviations for the amino acid residues are as follows: A, Ala; C, Cys; D, Asp; E, Glu; F, Phe; G, Gly; H, His; I, Ile; K, Lys; L, Leu; M, Met; N, Asn; P, Pro; Q, Gln; R, Arg; S, Ser; T, Thr; V, Val; W, Trp; and Y, Tyr.
 15. K. Irie *et al.*, *Mol. Cell. Biol.* **13**, 3076 (1993).
 16. B. Dérjard *et al.*, *Science* **267**, 682 (1995).
 17. D. R. Alessi *et al.*, *EMBO J.* **13**, 1610 (1994).
 18. Z. Galcheva-Gargova, B. Dérjard, I.-H. Wu, R. J. Davis, *Science* **265**, 806 (1994); J. Han, J.-D. Lee, L. Bibbs, R. J. Ulevitch, *ibid.*, p. 808.
 19. J. Rouse *et al.*, *Cell* **78**, 1027 (1994); I. Sánchez *et al.*, *Nature* **372**, 794 (1994).
 20. A. B. Vojtek, S. M. Hollenberg, J. A. Cooper, *Cell* **74**, 205 (1993).
 21. S. G. Oliver *et al.*, *Nature* **357**, 38 (1992).
 22. Strains used in Fig. 2, A and B, were as follows: wild-type = TM100 (*MATa ura3 leu2 trp1*); *pbs2Δ* = TM260 (*MATa ura3 leu2 trp1 pbs2::LEU2*); other strains are all derivatives of TM222 (*MATa ura3 leu2 trp1 his3*) that have the indicated combinations of *ssk2Δ* (*ssk2::URA3*), *ssk22Δ* (*ssk22::LEU2*), and *sho1Δ* (*sho1::TRP1*).
 23. We constructed the *pbs2^{K/M}* (Lys³⁸⁹ to Met) and *pbs2^{S/A T/A}* (Ser⁵¹⁴ to Ala; Thr⁵¹⁸ to Ala) mutant alleles by sequential polymerase chain reactions. The *PBS2⁺*, *pbs2-13*, *pbs2^{K/M}*, and *pbs2^{S/A T/A}* alleles were cloned into pRS317 (vector; *LYS2⁺* marker) [R. S. Sikorski and J. D. Boeke, *Methods Enzymol.* **194**, 302 (1991)]. These plasmids were transformed into each of the indicated host strains in Fig. 3. All host strains were isogenic to TM334 (*MATa ura3 leu2 trp1 his3 lys2 pbs2::HIS3*), into which various combinations of *ssk2Δ* (*ssk2::URA3*), *ssk22Δ* (*ssk22::LEU2*), and *sho1Δ* (*sho1::TRP1*) mutant alleles were introduced by genetic crosses.
 24. H. Yu *et al.*, *Cell* **76**, 933 (1994).
 25. The SH3 domain of Sho1p (amino acid positions 295 to the COOH-terminus) was cloned into a *LexA* DNA binding domain plasmid pBTM116 to create pLexA-SHO1(SH3). DNA segments corresponding to amino acid positions 13 (Xcm I site) to the COOH-terminus of wild-type *PBS2* and *pbs2-13* were cloned into a *GAL4* activation domain vector pACT2 [T. Durfee *et al.*, *Genes Dev.* **7**, 555 (1993)] to generate pACT-*PBS2⁺* and pACT-*pbs2-13*, respectively. Either pLexA-SHO1(SH3) or pLexA-RAS^{V12} was co-transformed with one of the pACT plasmids into the L40 reporter strain (20). Transformant cells (~5 × 10⁶) were spotted onto a YEPD plate, and after 5 hours at 30°C the cells were copied onto a nitrocellulose membrane. β-Galactosidase activity was visualized with the use of x-gal as described (20).
 26. We thank E. Brown and T. Thai for their excellent technical assistance, M. Streuli, S. Wurgler-Murphy, and N. X. Krueger for plasmids and comments on the manuscript, F. Winston, K. Dollard, S. J. Elledge, J. A. Cooper, K. Matsumoto, and R. D. Kolodner for yeast strains, plasmids, and libraries, and T. Ernst for synthesis of oligonucleotides. Plasmid pBTM116 was from P. Bartel and S. Fields. Supported by grants from NIH to H.S. and a postdoctoral fellowship from Sandoz to T.M.

17 March 1995; accepted 16 May 1995

AAAS–Newcomb Cleveland Prize

To Be Awarded for a Report, Research Article, or an Article Published in *Science*

The AAAS–Newcomb Cleveland Prize is awarded to the author of an outstanding paper published in *Science*. The value of the prize is \$5000; the winner also receives a bronze medal. The current competition period began with the 2 June 1995 issue and ends with the issue of 31 May 1996.

Reports, Research Articles, and Articles that include original research data, theories, or syntheses and are fundamental contributions to basic knowledge or technical achievements of far-reaching consequence are eligible for consideration for the prize. The paper must be a first-time publication of the author's own work. Reference to pertinent earlier work by the author may be included to give perspective.

Throughout the competition period, readers are

invited to nominate papers appearing in the Reports, Research Articles, or Articles sections. Nominations must be typed, and the following information provided: the title of the paper, issue in which it was published, author's name, and a brief statement of justification for nomination. Nominations should be submitted to the AAAS–Newcomb Cleveland Prize, AAAS, Room 924, 1333 H Street, NW, Washington, DC 20005, and **must be received on or before 30 June 1996**. Final selection will rest with a panel of distinguished scientists appointed by the editor-in-chief of *Science*.

The award will be presented at the 1997 AAAS annual meeting. In cases of multiple authorship, the prize will be divided equally between or among the authors.